Zakaria Layate[1]*,
Tahar Bahi[2]
Salima Lekhchine[3],
Meziane Kaci[1]

J. Electrical Systems 21-1 (2025): 102-115

Regular paper

Energy Management of Integrated Batteries in Grid-connected Photovoltaic System

Journal of Electrical Systems

Addressing the global challenges of rising energy demands and the pursuit of sustainable solutions, the integration of batteries within grid-connected photovoltaic (PV) systems emerges as a highly effective strategy for improving energy efficiency. This study proposes an innovative framework that combines advanced energy storage technologies with PV systems to ensure a steady and reliable flow of electric power. The system is designed to intelligently distribute electricity between the PV array, the energy storage unit, the load, and the single-phase grid. By leveraging solar energy harnessed by PV panels, surplus energy is stored in batteries for later use, particularly during periods of reduced sunlight or heightened energy demand. The inclusion of a battery energy storage system (BESS) not only enhances grid stability but also maximizes overall system performance, leading to reduced operational costs and a smaller environmental footprint. Through mathematical modeling and real-time performance analysis, the study evaluates the system s behavior under diverse conditions, such as variations in solar irradiance, ambient temperature, and energy consumption patterns. The results highlight a notable improvement in the reliability and efficiency of energy distribution, particularly in rural and underserved regions. This research contributes to the advancement of sustainable energy management by offering a scalable and flexible solution that fosters environmental conservation and energy autonomy.

*Keywords:*Photovoltaic, Electrical grid, Energy storage, MPPT optimization, Phase Locked Loop, Power quality.

1. Introduction

The rapid depletion of conventional energy resources, coupled with increasing energy demands and escalating environmental concerns, underscores the urgency of developing innovative, efficient, and sustainable technologies. Among various renewable energy alternatives, solar energy emerges as a clean, sustainable, and highly versatile solution. Photovoltaic (PV) systems, which convert solar energy into electricity, provide a cost-effective option for diverse applications, including street lighting, water heating, and agricultural systems [1–3]. Expanding the adoption of renewable energy technologies is essential to combat the effects of climate change and global warming, particularly in areas with limited access to traditional power grids [4, 5].

A significant application of PV technology lies in grid-connected systems equipped with energy storage, which are especially valuable in remote and off-grid regions. In such areas, PV systems with integrated battery storage offer a reliable and eco-friendly alternative to conventional energy solutions. These systems are known for their low

* Corresponding author: Zakaria Layate, E-mail: z.layate@univ-dbkm.dz
[1] *Department of Electrical Engineering, Faculty Sciences and Technologies, Khemis Miliana University, Algeria.*
[2] *Department of Electrical Engineering, Faculty of Technologies, Annaba University, 23000, Algeria.*
[3] *Department of Electrical Engineering, Faculty Sciences and Technologies, Skikda University, 21000, Algeria.*

maintenance requirements, energy efficiency, and substantial long-term cost benefits. Incorporating energy storage units, such as batteries, ensures uninterrupted power availability, even during periods of reduced solar irradiance or night time [6, 7].

Research has highlighted the transformative potential of PV systems combined with energy storage, particularly for improving energy access in rural regions, including developing countries. For instance, in sub-Saharan Africa, these systems are increasingly supported by governments, non-governmental organizations (NGOs), and development agencies to enhance energy accessibility. However, achieving sustainable operation of these systems necessitates meticulous monitoring and optimization [8].Numerous studies have explored the optimal design and sizing of PV systems with energy storage to enhance their efficiency and cost-effectiveness. Key factors considered include solar radiation availability, energy consumption patterns, and costs related to component purchase, maintenance, and replacement [9–12]. Additionally, intelligent optimization methods have significantly boosted the performance of such systems, ensuring they meet user energy needs while minimizing environmental impacts and operational expenses [13–15].

This paper focuses on the analysis of various battery charging and discharging scenarios in a grid-connected PV system with integrated energy storage. The inclusion of batteries as storage components is crucial for maintaining a stable energy supply during periods of reduced solar input or at night. By studying multiple charging and discharging scenarios, the research aims to enhance system performance and efficiency, ensuring it meets user energy demands while minimizing costs and environmental footprint. The study also emphasizes the benefits of PV systems with energy storage, such as reduced environmental impact, economic savings, and their capacity to improve energy access in underserved and remote areas. Furthermore, the challenges related to the implementation of these systems, including the need for regular monitoring and maintenance, are addressed to ensure their durability and sustainability.

The remainder of this paper is structured as follows: Section 2 details the overall system design, converter topologies, and control methodologies. Section 3 presents the system management algorithm, while Section 4 discusses the results. Finally, Section 5 concludes the paper.

2. Overall system modelling and design

The block diagram presented in Fig. 1 illustrates the grid-connected solar PV system developed in this study. This system consists of key components, including solar PV modules, a DC-DC boost converter, and a DC-AC inverter that facilitates grid connection and enables power delivery to the grid. The synchronization circuit is responsible for generating control signals for the gate drive circuit, ensuring seamless integration with the grid. For single-phase grid synchronization, a Phase Locked Loop (PLL)-based technique was utilized, enabling precise alignment of the system with grid parameters.

To maximize the energy harvested from the solar PV modules, incremental Maximum Power Point Tracking (MPPT) algorithms were employed. These algorithms dynamically adjust the operating point of the PV modules to extract maximum power under varying solar irradiance and temperature conditions.

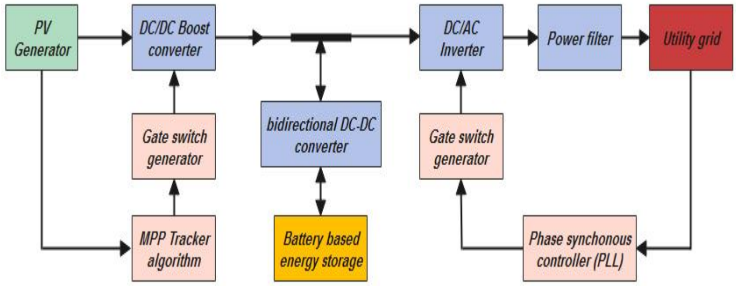

Fig. 1. Block diagram of grid-connected solar PV System

In the subsequent subsections, we provide a detailed model of the main components of the photovoltaic system under consideration. Each component's role in the energy conversion process and its contribution to the overall system performance are thoroughly analysed.

2.1 PV Unit Model

The equivalent electrical circuit of a photovoltaic (PV) cell, depicted in Fig. 2, adopts the single-diode model [16–18], which accurately represents the real behavior of the cell.

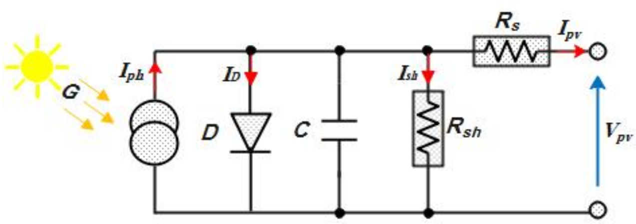

Fig. 2. Equivalent Electrical Circuit for a Photovoltaic Cell

This model comprises a photocurrent source (I_{Ph}), a diode (D), a series resistor (R_s), and a shunt resistor (R_{sh}). The series resistance (R_s) accounts for losses due to the Joule effect, while the shunt resistance (R_{sh}) represents leakage currents between the upper grid and the rear contact, typically much greater than (R_s) [18].

To incorporate the dynamic response of the PV cell under varying irradiance conditions, a capacitance is added in parallel with the diode. This capacitance simulates the charge storage effects of the cell, considering the significant influence of temperature and solar irradiation on the PV array's output characteristics [19].

The power output generated by the PV module can be expressed mathematically as follows [20, 21]:

$$P_{PV}(G_o, T_o) = P_{stc} \,.\, f_{ad} \,.\, G_o[1 + \delta\,(T_o - 25)] \quad (1)$$

Where;

$P_{stc}[kW]$: Rated output power of the PV module under Standard Test Conditions (STC).

f_{ad} : Adjustment factor accounting for real-world energy losses, such as soiling, shading, mismatches, wiring, and other practical inefficiencies.

$G_o[W/m^2]$ and $T_o[°C]$: Operating solar irradiance and temperature, respectively.

$\delta[\%/°C]$: Temperature coefficient describing the impact of temperature on PV power output.

The output current (I_{Pv}) and voltage (V_{Pv}) of the PV cell can be formulated as follows:

$$I_{PV} = I_{Ph} - I_D - I_{sh} \tag{2}$$

$$V_{PV} = V_D - R_s I_{PV} \tag{3}$$

The currents through the diode (I_D) and the shunt resistance (I_{sh}) are derived using the Shockley diode equation and Ohm's law, respectively:

$$I_d = I_0[\, e^{\left(\frac{qV_d}{nkT}\right)} - 1] \tag{4}$$

$$I_{sh} = \frac{V_d}{R_{sh}} \tag{5}$$

By substituting these equations, the expression for the photocurrent can be refined as:

$$I_{pv} = I_{ph} - I_0 \left[e^{\left(\frac{q(V_{pv} + I_{pv} R_S)}{nkT}\right)} - 1 \right] - \frac{V_{pv} + I_{pv} R_s}{R_{sh}} \tag{6}$$

Finally, considering both series and parallel PV cells, the generalized form becomes:

$$I_{PV} = I_{ph} - I_{sat} \left(e^{\frac{q(V_{pv} + R_S . I_{pv})}{n.K.TNs}} - 1 \right) - q\, N_p \left(\frac{V_{pv} + R_S . I_{pv}}{R_{sh}\, R_s} \right) \tag{7}$$

This formulation captures the key parameters influencing PV module behavior, providing a comprehensive foundation for further analysis and optimization.

2.2 Boost Converter Model

The electrical schematic of the boost converter, illustrated in Fig. 3, highlights its core components and functional design.

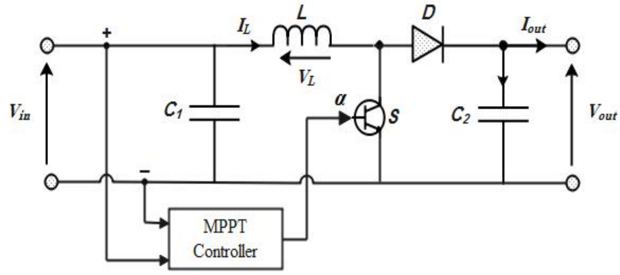

Fig. 3. Electrical Circuit of the Boost Converter

The boost converter acts as an interface between the energy source and the load. It primarily comprises an inductor(L), a static switch (S) controlled by the duty cycle(α), a diode(D), and a capacitor(C_2). The duty cycle (α) is governed by the Maximum Power Point Tracking (*MPPT*) control algorithm to maximize energy extraction from the source. The insulated-gate bipolar transistor (*IGBT*) switch operates under the influence of(α), enabling regulation of the output voltage [22].

At steady-state conditions, the relationship between the input voltage (V_{in}) and the output voltage (V_{out}) is expressed as follows [23, 24]:

$$V_{out} = V_{in}/(1-\alpha) \tag{8}$$

Here, the duty cycle (α) ranges from 0 to 1, calculated as:

$$\alpha = 1 - (V_{in}/V_{out}) \quad (9)$$

The output voltage (V_{out}) and output load current (I_{out}) can be determined using these equations [25]-[26]:

$$V_{out} = (V_{DC} - L.I_L)/(1 - V_{DC}^*) \quad (10)$$

$$I_{out} = I_L(1 - V_{DC}^*) - C \,.\, V_{out} \quad (11)$$

Where,

V_{DC} : Boost converter input voltage; V_{DC}^* : Input reference voltage and I_L : Inductor current.

The values of the boost inductor (L) and capacitance (C) are determined by the following expressions [27]:

$$L = V_{DC}(V_{out} - V_{DC})/(f_s \,.\, \Delta I_{out} \,.\, V_{out}) \quad (12)$$

$$C = I_{out} \,.d/f_s \,.\Delta V_{out} \quad (13)$$

Here, ΔI_{out} and ΔV_{out} : represent the ripple in output current and voltage, respectively, f_s :switching frequency; d:duty ratio.
The design of the boost converter of this study is based on the parameters listed in Table 1.

Table 1. Boost system parameters

Symbol	Quantity	Value
L	Input inductor	0.1164 [H]
C_{out}	Output capacitor	0.5 [μF]
F_s	Switching frequency	10 [KHz]

2.3 Maximum Power Point Tracker

The Perturb and Observe (P&O) algorithm is employed to adjust the PV output voltage, ensuring it reaches the Maximum Power Point (MPP) [28]. This method involves periodically perturbing the module voltage [29]. As shown in Fig. 4 below, an increase (or decrease) in voltage results in a corresponding increase (or decrease) in power. To achieve the MPP, power should be increased by maintaining a constant perturbation. Conversely, when power decreases, the perturbation direction is reversed proportionally [30].

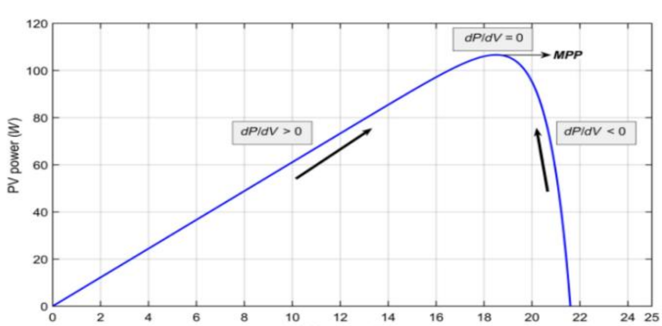

Fig. 4. P-V Curve for the Perturb and Observe (P&O) Algorithm

This method examines the change in power (dP) of the PV system in response to a change in PV cell voltage(dV). When dP/dV is positive, the operating point is on the left side of the MPP. This process continues until dP/dV reaches zero, as illustrated below:

$dP/dV = 0$ at MPP (14)

$dP/dV > 0$ on the left side of MPP (15)

$dP/dV < 0$ on the right side of MPP (16)

The Incremental Conductance (INC) method operates by adjusting the photovoltaic power in relation to its voltage. The MPP is attained when the derivative of the power with respect to voltage equals zero [31, 32]:

$$dP/dV = d(V.I)/dV = I + V.(dI/dV) \quad (17)$$

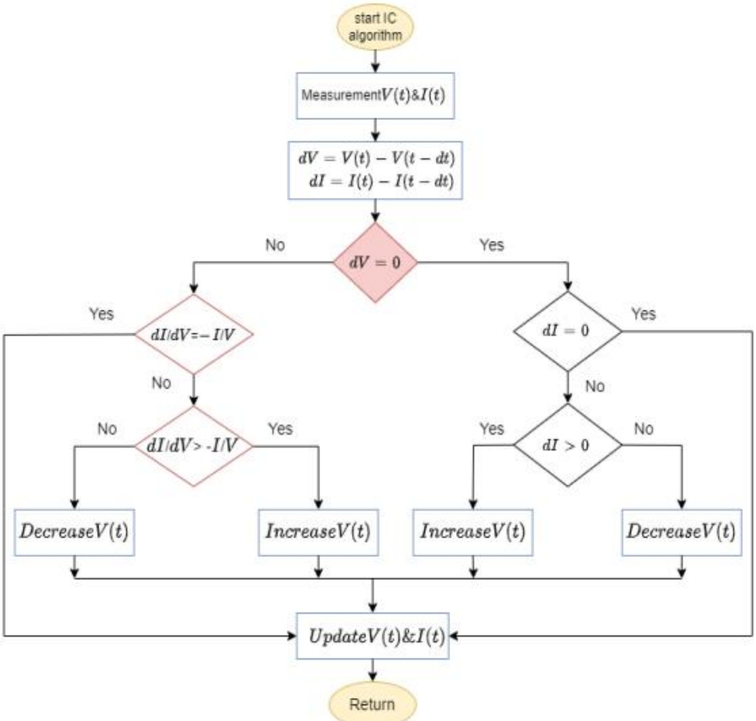

In this study, a single lithium-ion phosphate battery is utilized, with parameters listed in figure 7. Key characteristics, such as open-circuit voltage and internal resistance, are modeled as functions of the State of Charge (SOC) using the internal resistance method [33].

$$P_{battery} = P_B + P_L + P_B + R_B.I_B{}^2 \quad (19)$$

Where,
$P_{battery}$: Internal rated power of the battery; P_B : Terminal battery power; P_L : Load power; I_B : Total battery current; R_B : Equivalent internal resistance of the battery.
The rate at which the battery's capacity decreases during the charge-discharge cycle is influenced by temperature and current. The point at which the battery's capacity drops to 80% of its initial value is termed the end of lifespan (EOF) [34]. The decline in battery life can be expressed as:

$$Q_{loss} = \beta \, . \, e^{-\frac{E_A}{R.T_{battery}}} \, . \, A_h^z \qquad (20)$$

Where,

Q_{loss} : Capacity loss; β : Exponential factor.
E_A, β, $T_{battery}$, A_h and z : Represent activation energy, gas constant, battery temperature, ampere-hour throughput, and power law factor, respectively.
Under certain assumptions, the theoretical lifespan of the battery can be defined by [35]:

$$\lambda_{min} = \int_0^{EOL} |I_{Bmin}(t)| . dt \qquad (21)$$

In this equation, λ_{min} represents the battery's lifespan, and $I_{Bmin}(t)$ is the minimum current at time "t". This formulation accounts for a 20% allowable capacity loss.

The service factor, related to the battery's rating, is defined by equation (23):

$$\lambda_{min} = \left[\frac{20}{\beta . e^{\frac{\alpha + I_{Bmin}}{R.T_{min}}}} \right]^{\frac{1}{z}} \qquad (22)$$

The battery operates at 25°C, as it is well-established that temperature control systems facilitate more gradual cell aging. The thermal management system heats and cools the battery, regulating current flow during operation. Then, the battery SOC is given by:

$$SOC\% = \frac{\left(-V_{oc} - \sqrt{\left(V_{oc}^2 - 4 \, . \, R_B \, . \, P_B \right)} \right)}{2 \, . \, q_B \, . \, R_B} \qquad (23)$$

Where,

V_{oc} and q_B represent the opencircuit voltage and capacity of the battery, respectively.

The system operates in two modes: charge and discharge. The battery controller circuit used in MatLab/Simulink, along with its characteristics, is illustrated in Fig. 6 and detailed in parameters MatLab window by Fig. 7;

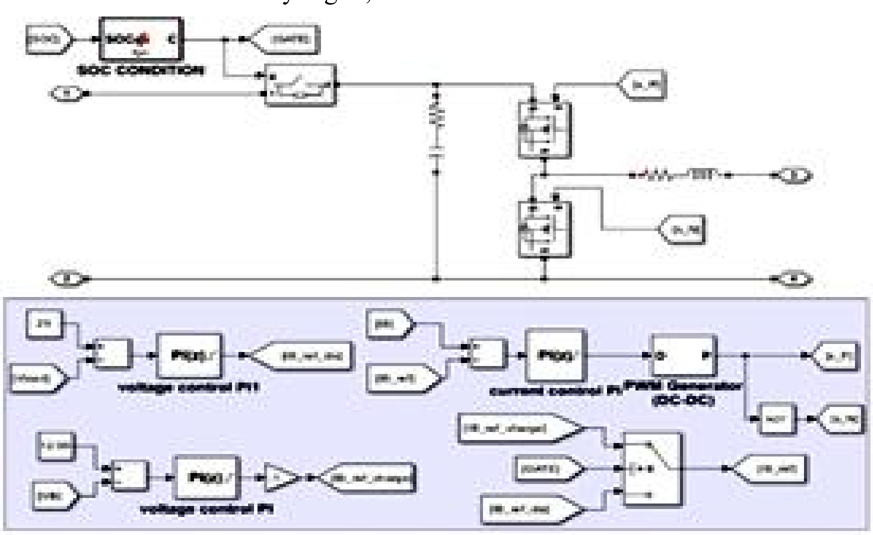

Fig. 6. Battery SOC controller in MatLab/Simulink

Additionally, the nominal discharge current, which represents the maximum current a battery can safely discharge, is significantly influenced by the State of Charge (SOC) and Depth of Discharge (DOD) of the battery. Understanding the nominal discharge current enables better management of battery performance, as illustrated in Fig. 7. This understanding helps optimize the battery's operating conditions under specific circumstances.

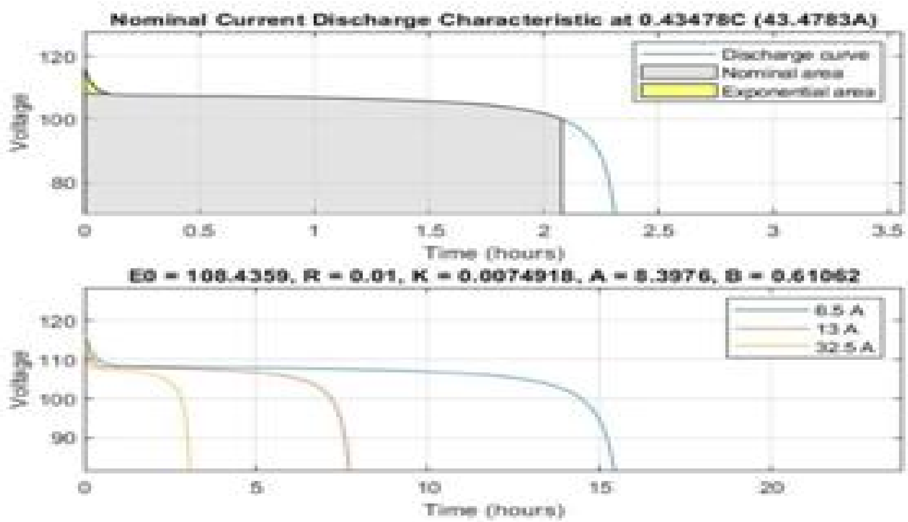

Fig. 7. Battery Nominal Current Discharge Characteristics

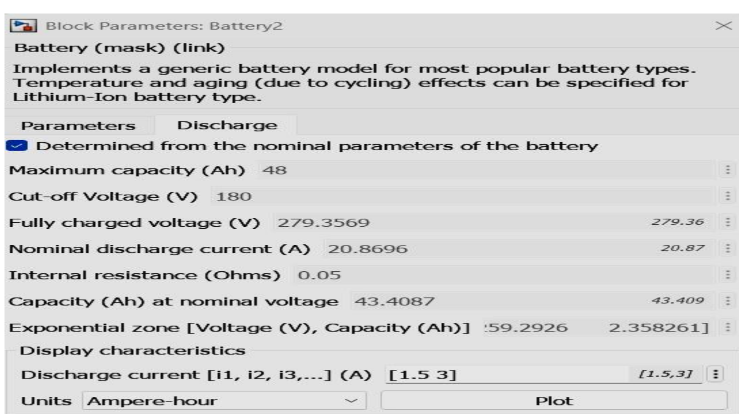

Fig. 8. Essential battery parameters

3. Simulation Results and Analysis

To evaluate the performance of the overall power chain, essential parameters, as listed in MatLab/Simulink parameters window (figure 9), were considered. The power and current characteristics as functions of the photovoltaic generator voltage are illustrated in Figures 10(a) and 10(b). For this evaluation, MatLab/Simulink software was employed.

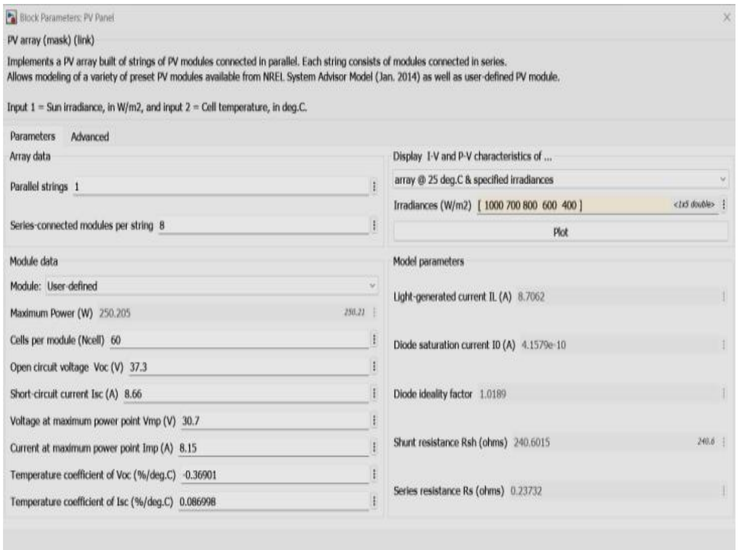

Fig. 9. PV system's essential parameters

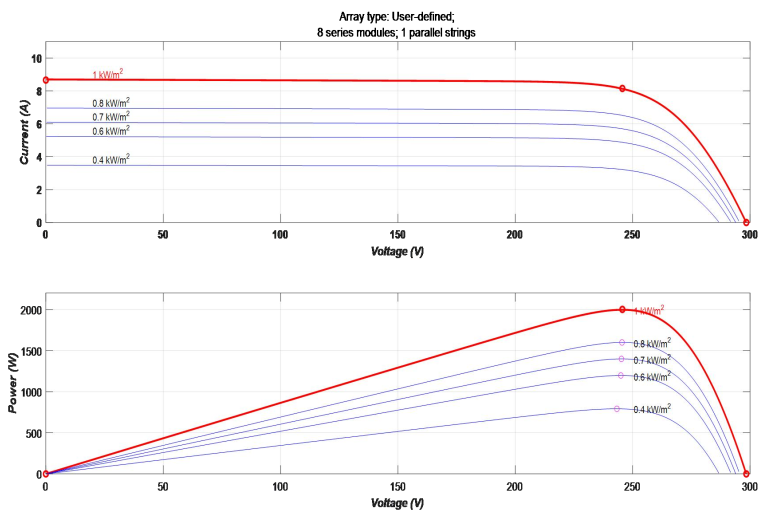

Fig. 10. Power and Current Characteristics of the Photovoltaic Generator Voltage
$I_{PV} = f(V_{PV})$ and $P_{PV} = f(V_{PV})$

For each irradiation level, it can be observed that the MPPT achieves maximum power, as detailed in Table 2. Since changes in irradiation are inevitable in real-world scenarios, the objective is to ensure that the MPPT consistently extracts the global maximum power under varying conditions.

Table 2. Coordinates of the Maximum Power Points (MPP)

$G\ [W/m^2]$		400	600	700	800	1000
MPP	V_{pv_max}	243,2	244,95	245,21	245	245
	P_{pv_max}	792,2	1197,72	1399,38	1600	2001,64

We will begin by examining the values of the GPV under varying irradiation effects at a fixed temperature of$T = 25°C$, as shown in Figure 11. Our initial focus will be on assessing the performance and effectiveness of the Incremental Conductance (INC) optimization technique used to regulate the overall maximum power point (MPP) achievable by a PV array in the presence of sudden changes in irradiance, which significantly influence the power produced by the photovoltaic array.

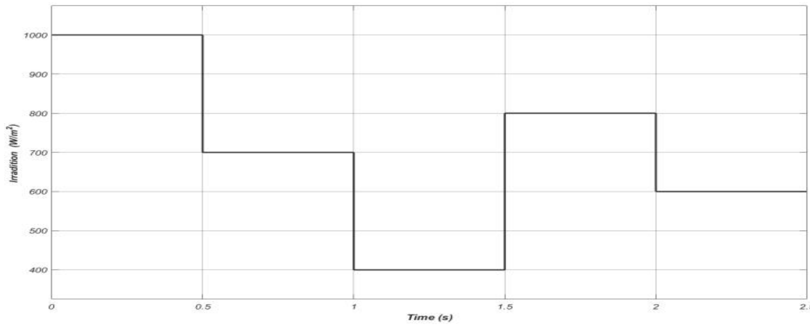

Fig. 11. Profile of Irradiation Variation

To evaluate the system's performance under varying irradiation profiles, simulations were conducted. The results, particularly the photovoltaic voltage, current, and power, are illustrated in Figure 12. Additionally, the same magnitudes at the DC bus level and the battery's State of Charging (SOC) are presented in Figures 13 and 14, respectively. Finally, Figure 15 depicts the various currents, including those of the boost converter, the reversible converter for battery charging and discharging, the inverter input current, and the sum of the DC bus currents at the bottom of the figure. Analysing Figure 13 reveals that the MPPT control effectively achieves its objective, as the GPV generates power closely corresponding to the irradiation levels indicated in Table 2 and confirmed by the results in Table 3. Furthermore, the values at the DC bus level (Figure 15) are justified by considering the load power and the power produced by the GPV. Figure 14 demonstrates the different battery operation modes deduced at each time interval (refer to the last column of Table 3), which aligns well with the current behavior analysis shown in Figure 15.

Table 3. Power under each irradiation level

Time laps (s)	$G\ [W/m^2]$	$V_{PV}[V]$	$P_{PV}[W]$	*Battery state*
0 to 0.5	1000	245,6	2000	Charging
0.5 to 1	700	245	1400	Maintaining
1 to 1.5	400	243.6	779	Discharging
1.5 to 2	800	244.8	1580	charging
2 to 2.5	600	245.1	1200	Discharging

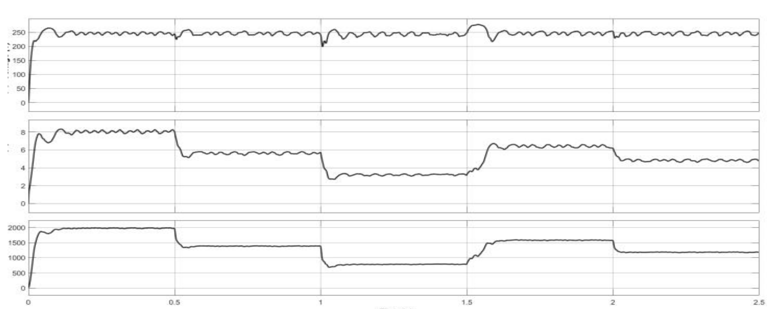

Fig. 12. GPV voltage, current and power

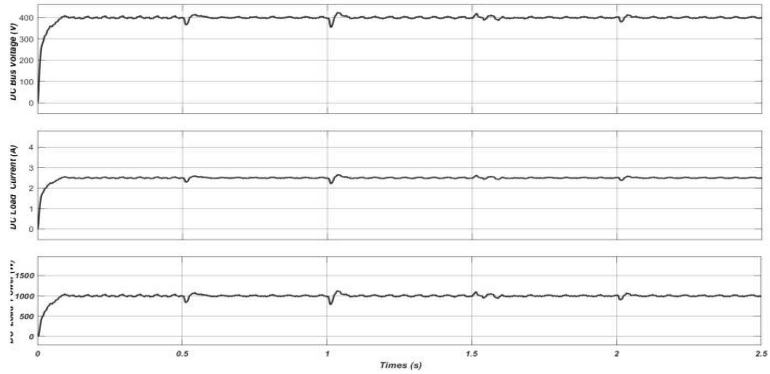

Fig. 13. DC bus voltage, current and power

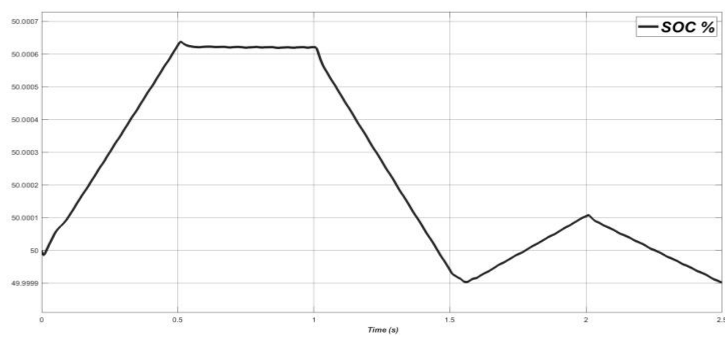

Fig. 14. DC bus voltage, current and power

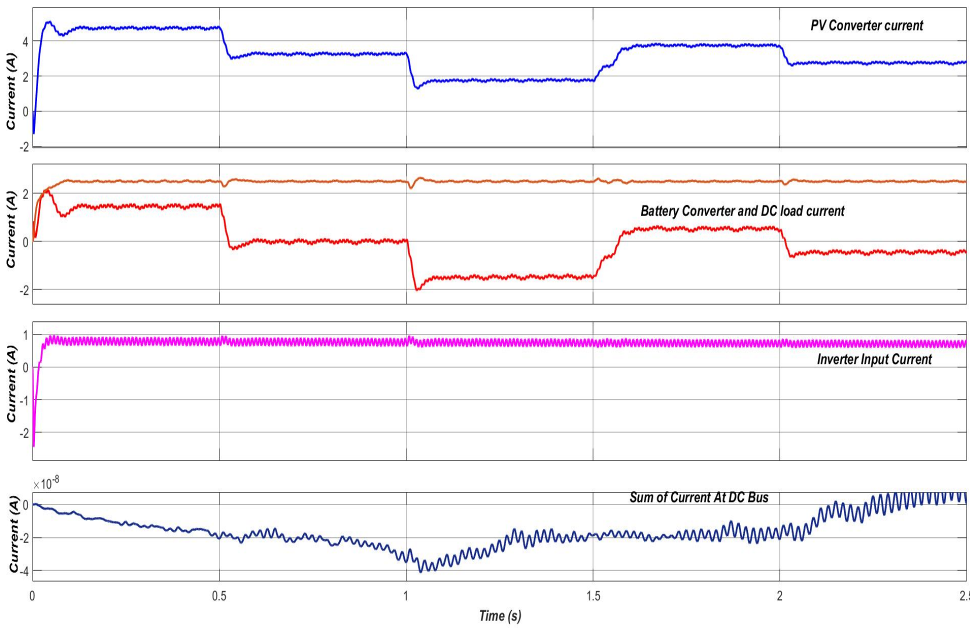

Fig. 15. Boost, reversible AC converter, battery and the sum of DC bus currents

4. Conclusion

This study presents a comprehensive framework for integrating batteries into grid-connected photovoltaic (PV) systems, highlighting the substantial benefits of combining advanced energy storage technologies with solar power generation. By meticulously analyzing various charging and discharging scenarios, the research demonstrates the potential of battery energy storage systems (BESS) to stabilize the grid and enhance the overall efficiency and reliability of energy distribution, especially in rural and underserved areas.

The proposed system optimizes energy management through the implementation of incremental Maximum Power Point Tracking (MPPT) algorithms, which effectively regulate the power output of the PV array under fluctuating irradiance conditions. The utilization of a boost converter and a well-designed battery management system further ensures the seamless conversion and storage of solar energy, thus enabling continuous power supply during periods of low sunlight or high demand.

Simulation results validate the system's performance, showcasing its ability to maintain stable voltage and current levels while meeting the energy demands of the load. The analysis confirms that the GPV, coupled with the BESS, consistently achieves the maximum power point (MPP) under varying irradiation profiles, thereby maximizing energy harvest and minimizing environmental impact.

Overall, this research contributes to the advancement of sustainable energy management practices by providing a scalable and adaptable solution that promotes energy self-sufficiency and environmental stewardship. The findings underscore the importance of integrating intelligent optimization methods and robust energy storage mechanisms in renewable energy systems to address the global challenges of rising energy demands and environmental sustainability.

References

[1] O. Noureldeen and A. M. A. Ibrahim, "Performance Analysis of Grid Connected PV/Wind Hybrid Power System During Variations of Environmental Conditions and Load", International Journal of Renewable Energy Research, vol. 8, no. 1, pp. 208-220, 2018.

[2] O. Djoudi , S. L. Belaid , S. Tamalouzt, D. Ziane , A. Houari, A. Saim , "An intelligent demand side management for stand-alone AC microgrid based on wind- DFIG/battery hybrid system", J. Electrical Systems 20-4 , pp: 382-393, 2024.

[3] A. B. Oskouei, M. R. Banaei and M. Sabahi, "Hybrid PV/wind system with quinary asymmetric inverter without increasing DC-link number", Ain Shams Engineering Journal, vol. 7, no. 2, pp. 579-592, 2016.

[4] A. K. Aliyu, B. Modu, C.W. Tan, "A review of renewable energy development in Africa: A focus in South Africa, Egypt and Nigeria", Renewable and Sustainable Energy Reviews, vol. 81, pp. 2502-2518, 2018.

[5] H. I. Hazim, K. A. Baharin, C.K. Gan and A.H. Sabry, "Techno-economic optimization of photovoltaic (PV) inverter power sizing ratio for grid-connected PV systems", Results in Engineering, vol. 23, pp. 102580, 2024.

[6] M. H. Nehrir, C. Wang, K. Strunz, H. Aki, R. Ramakumar, J. Bing, Z. Miao and Z. Salameh, "A review of hybrid renewable/alternative energy systems for electric power generation: Configurations, control, and applications", IEEE transactions on sustainable energy, vol. 2, no. 4, pp. 392-403, 2011.

[7] S. A. Belfedhal, E. L. Berkouk and Y. Messlem, "Analysis of grid connected hybrid renewable energy system", Journal of Renewable and Sustainable Energy, vol. 11, no. 1, 2019.

[8] G. Ren, J. Wang, Y. Li and G. Zhang, "Power distribution optimization of a fully active hybrid energy storage system configuration for vehicular applications", Journal of Industrial Information Integration, 2023, vol. 33, pp. 100459, 2023.

[9] S. Lekhchine, T. Bahi, "Management and control of a solar pumping system", J. Electrical Systems 20-4, pp: 495-506, 2024.

[10] S. H. Nengroo, M. U. Ali, A. Zafar, S. Hussain, T. Murtaza, M. J. Alvi, K. V. G. Raghavendra and H. J. Kim, " An optimized methodology for a hybrid photo-voltaic and energy storage system connected to a low-voltage grid", Electronics, vol. 8, no. 2, pp. 176, 2019.

[11] A. A. Khan, A. F. Minai, R. K. Pachauri and H. Malik, "Optimal sizing, control, and management strategies for hybrid renewable energy systems: A comprehensive review", Energies, vol. 15, no. 17, pp. 6249, 2022.

[12] G. A. D Ibrahim, "Efficient Use of Sun Energy in Plant Production in One and Half Million Feddan Regions (Case Study of the Frafra Oases)", Journal of the Advances in Agricultural Researches, vol. 27, no. 2, pp. 425-441, 2022.

[13] A. Jafar-Nowdeh, M. Babanezhad, S. Arabi-Nowdeh, A. Naderipour, H. Kamyab, Z. Abdul-Malek, and V. K. Ramachandaramurthy, "Meta-heuristic Matrix Moth–flame Algorithm for Optimal Reconfiguration of Distribution Networks and Placement of Solar and Wind Renewable Sources Considering Reliability", Environmental Technology & Innovation, vol. 20, pp. 101118, 2020.

[14] G. Shafiullah, T. Masola, R. Samu, R. M. Elavarasan, S. Begum, U. Subramaniam, M. F. Romlie, M. Chowdhury, and M. T. Arif, "Prospects of hybrid renewable energy-based power system: A case study, post analysis of Chipendeke Micro-Hydro, Zimbabwe",IEEE Access, vol. 9, pp. 73433–73452, 2021.

[15] S. Lekhchine, A. Boukerche, T. Bahi, "Study of optimization methods for monitoring the maximum power of a solar system", Algerian Journal of Renewable Energy and Sustainable Development, vol. 3, no. 2, pp. 157-165, 2021.

[16] J. C. León Gómez, S. E. De León Aldaco and J. Aguayo Alquicira, " A review of hybrid renewable energy systems: architectures, battery systems, and optimization techniques. Eng, vol. 4, no. 2, pp. 1446-1467, 2023.

[17] Z. Layate, B.Tahar, L.Salima, "Dynamic flow control of a photovoltaic pumping system-based asynchronous induction motor",International Journal of Nonlinear Dynamics and Control, vol. 1, no. 3, pp. 255-270, 2019.

[18] Y. Izgheche, T. Bahi, A. Lakhdara, "Intelligent Power Management Control for Hybrid Wind Solar Battery Systems Connected to Micro-Grids", Journal Européen des Systèmes Automatisés, vol. 57, no. 4, 2024.

[19] V. Yarlagadda, G. P. Ambati, C. R. Reddy, D. R. Kumar, J. S. Rao, B. V. S. Kumari, "Realization of Small Scale Models of FCATS Devices and its Optimization in Power Systems using Stability Indices and Particle Swarm Optimization", J. Electrical Systems 19-1, pp: 53-63, 2023.

[20] D. Bonkoungou, Z. Koalaga, and D. Njomo, " Modelling and Simulation of photovoltaic module considering single-diode equivalent circuit model in MATLAB", International Journal of Emerging Technology and Advanced Engineering, vol. 3, no. 3, pp. 493-502, 2013.

[21] V. Jha, "Comprehensive modeling and simulation of PV module and different PV array configurations under partial shading condition", Iranian Journal of Science and Technology, Transactions of Electrical Engineering, vol. 46, no. 2, pp. 503-535, 2022.

[22] R. S. Inomoto, J. R. B. de Almeida Monteiro, and A. J. Sguarezi Filho, "Boost converter control of PV system using sliding mode control with integrative sliding surface", IEEE Journal of Emerging and Selected Topics in Power Electronics, vol. 10, no. 5, pp. 5522-5530, 2022.

[23] C. Jiang, "African vulture optimized RNN algorithm maximum power point tracking (MPPT) controller for photovoltaic (PV) system", Measurement: Sensors, vol. 36, pp. 101392, 2024.

[24] N. Subhani, R. Kannan, M. A. Mahmud and M. F. Romlie, "Performance analysis of a modernized Z-source inverter for robust boost control in PV power conditioning systems", Electronics, vol. 8, no. 2, pp. 139, 2019.

[25] H. A. Mosalam, R.A. Amer and G. A. Morsy, "Fuzzy logic control for a grid-connected PV array through Z-source-inverter using maximum constant boost control method", Ain Shams Engineering Journal, vol. 9, no. 4, pp. 2931-2941, 2018.

[26] S. Manna, D. K. Singh, A. K. Akella, H. Kotb, K. M. AboRas, H. M. Zawbaa and S. Kamel, " Design and implementation of a new adaptive MPPT controller for solar PV systems", Energy Reports, vol. 9, pp. 1818-1829, 2023.

[27] R. Kahani, M. Jamil, M. T. Iqbal, "Direct model reference adaptive control of a boost converter for voltage regulation in microgrids", Energies, vol. 15, no. 14, pp. 5080, 2022.

[28] S. M. Fatemi, M. S. Shadlu, S. Milad and A. Talebkhah, "Comparison of three-point P&O and hill climbing methods for maximum power point tracking in PV systems", IEEE 10th International Power Electronics, Drive Systems and Technologies Conference, pp. 764-768, 2019.

[29] S. Salman, X. Ai, Z. Wu, "Design of a P&O algorithm based MPPT charge controller for a stand-alone 200W PV system", Protection and control of modern power systems, vol. 3, no. 1, pp. 1-8, 2018.

[30] A. K. Podder, N. K. Roy, H. R. Pota, "MPPT methods for solar PV systems: a critical review based on tracking nature", IET Renewable Power Generation, vol. 13, no. 10, pp. 1615-1632, 2019.

[31] S. Bhattacharyya, S. Samanta and S. Mishra, "Steady output and fast tracking MPPT (SOFT-MPPT) for P&O and InC algorithms", IEEE Transactions on Sustainable Energy, vol. 12, no. 1, pp. 293-302, 2020.

[32] A. Lakhdara, T. Bahi, A. Moussaoui, "Study and Management of a Hybrid System Connected to The Network" J. Electrical Systems 18-2, pp: 163-172, 2022.

[33] C. Jamroen, P. Vongkoon, "The role of state-of-charge management in optimal techno-economic battery energy storage sizing for off-grid residential photovoltaic systems", Journal of Energy Storage, vol. 72, pp. 108246, 2023.

[34] M. Cheng, A. Ran, X. Zheng, X. Zhang, G. Wei, G. Zhou and H. Sun, "Sustainability evaluation of second-life battery applications in grid-connected PV-battery systems", Journal of Power Sources, vol. 550, pp. 232132, 2022.

[35] H. K. Salim, R. A. Stewart, O. Sahin and M. Dudley, "Systems approach to end-of-life management of residential photovoltaic panels and battery energy storage system in Australia", Renewable and Sustainable Energy Reviews, vol. 134, pp. 110176, 2020.